Application of optimal control for wind integrated power system

Nelson Dhanpal Chetty[1], Gulshan Sharma[2], Pitshou N. Bokoro[2], Manoj Kumawat[3]

[1]Department of Electrical Power Engineering, Durban University of Technology, Durban, South Africa
[2]Department of Electrical Engineering Technology, University of Johannesburg, Johannesburg, South Africa
[3]Department of Electrical Engineering, National Institute of Technology, Delhi, India

Article Info

ABSTRACT

This paper presents the modeling and application of an optimal controller for frequency and tie-line power stability for a two-area interconnected hydro-thermal power plant having tandem compound non-reheat turbines integrated with wind power generation having doubly fed induction generator (DFIG) wind turbines in each area. The power system is interconnected using AC tie-lines. The designed optimal controller was implemented and the system dynamic responses for three power system model states were obtained considering a 1% load fluctuation in one of the areas. The optimal control strategy presented in this paper depends on formulating an error value and finding the feedback gains corresponding to each state of the system, which are easily attainable as outputs. The analysis was undertaken and verified by calculating the performance index value, the closed ring real and imaginary values, finding the feedback gains, and through graphical simulations of the three system models under investigation. The output of the optimal controller was enhanced when the DFIG-based wind turbines were installed in each area combined with a superconducting magnetic energy storage (SMES) unit and a thyristor control phase shifter (TCPS).

Corresponding Author:

Gulshan Sharma
Department of Electrical Engineering Technology, University of Johannesburg
Johannesburg, South Africa
Email: gulshans@uj.ac.za

1. INTRODUCTION

One of the fundamental requirements of a power utility is to deliver reliable power to consumers with voltage and frequency fluctuations minimized within an acceptable range. To effectively achieve this, electrical management systems (EMS) are employed. Frequency management is an essential component in an EMS. In an interconnected system, effective operation requires the coordination of the load demand and related system fluctuations. As the load demand changes constantly from a pre-determined value, the operational point of the power system shifts. This may result in extremely undesirable frequency and tie-line power deviations within the power system and may extend into other interconnected areas. The frequency fluctuations of the power system affect the speed of the consumers' plants which may result in equipment failure. The frequency needs to be stable for normal operations of the system and normal operations of other systems within the interconnected system. Subsequently, frequency management strategies play a vital part in complex, multi-area power systems.

The main objective is to control the electrical yield of the generators to supply the constantly changing load demands. The control mechanism directs the controlled yield of generators within a control area in reaction to changes in system frequency, tie-line power deviations, and area control errors. This maintains the system's frequency and compatibility with other interconnected areas, within predetermined limits. Various strategies,

based on the classical control theory, have been proposed relating to the frequency stability of an interconnected system [1]–[4]. Controllers based on classical control theory are constrained to systems only having a single-input-single-output formulation. However, frequency stability is a multi-variable problem that can be solved using innovative control strategies such as optimal control techniques. Controllers based on optimal control strategies yield significantly better performance results compared to conventional controllers [5]–[9]. An optimal control strategy requires access to all system state variables. Practically it is virtually impossible to attain all the state variables. Techniques based on system state reconstruction could be employed to overcome this problem, but it is very costly and leads to additional complexities in the power system. The optimal control strategy depends on formulating an error value and finding the feedback gains corresponding to each state of the system which are easily attainable as outputs. The stability of the control action is evaluated through eigenvalue analysis in a closed ring [10]–[14].

There is global momentum in pursuing renewables, such as hydro, solar, and wind, for new capacity builds as sources of cheaper and cleaner energy to meet the ever-increasing energy demands. Of all the renewable sources, wind generation seems to be the most promising. The active characteristics of wind generators are very diverse compared to ordinary generators. The kinetic energy of wind generators is not accessible to support the system frequency when changes occur. This impediment is accentuated in power systems that have wind energy integrations. If the installed wind capacity is adequately accessible to supply acceptable inertial support, the unfavorable consequences of the load variabilities can be minimized [15]. With innovative developments, it is presently realistic for wind generators to partake in frequency control provisions in power systems. In the case of DFIGs, the inertia of the turbine is decoupled from the system, thereby generators do not react to frequency changes in the system. This is achieved by electronic controllers that act as an interface between the turbine and the grid. Few approaches have been detailed on the capacity of variable-speed wind turbines to participate in the frequency control of power systems. One approach is pitch and speed control (power reserve method), another approach is inertial control and there is also the communication approach [16]. An extra loop having inertial control with satisfactory gains is presented in [17]. The control loop is responsive to frequency variations in the system and supplies energy from DFIG back into the system with inertial support. A combination of static converters and pitch control is employed to develop the capacity of DFIGs to participate in frequency stability. The active power and rotor speed are balanced corresponding to the no-load extraction data to attain maximum power [18]. The active support of the DFIG in frequency stability is analyzed by frequency control feedback that reacts proportionally to frequency fluctuations and releases the kinetic energy stored in the blades of the turbine accordingly for frequency stabilization in the system [19]. A significant benefit of the DFIG is highlighted in [20]; the rotor side converter (RSC) deals with approximately 25% of the rated power which reduces losses, resulting in reduced cost compared to wind turbines that employ full-power converters. The investigation in [21] demonstrated that the power produced by the turbines that employ full-power converters is significantly lower, compared to the power produced by the DFIG-based wind turbines. Muñoz and Cañizares [22], the model analysis showed that the DFIG-based wind farm delivered better frequency responses when it replaced the conventional synchronous generators. The investigations in [23], [24] demonstrated the effective support of DFIG in maintaining desired system frequencies and improving power system stability.

To improve transmission reliability and power system stability, flexible alternating current transmission systems (FACTS) devices were developed to maintain system parameters at optimal operating values [25]. Assis et al. [26], FACTS devices are used to enhance the power transmission capabilities of electrical power systems, thereby eliminating the need to add new transmission lines to the network. The positive impact of FACTS devices used in power system stability, incorporating renewable energy generations is highlighted in [27]; they provide rapid compensation for, voltage, frequency, and active and reactive power variations to improve transient system stability. Energy storage devices such as the redox flow battery (RBF) and the battery energy storage system (BESS) are investigated with positive results [28]–[30]. However, the maintenance requirements, low discharge rates, and increased response times for power flow reversal are major disadvantages of the RBF and the BESS. These disadvantages drove the development of the superconducting magnetic energy storage (SMES) unit as an effective FACTS device, for frequency control and tie-line power stability in interconnected power systems. SMES units are desirable for LFC because of their rapid response times and their ability to simultaneously control active and reactive powers. The researces [31]–[33], investigate the performance of SMES units installed in interconnected power systems. Although the investigations demonstrate the positive impact of SMES, the investigations also revealed that SMES units only have a positive impact in the area in which the unit is installed and have negligible impact in other control areas. The researces [34]–[37], investigate the combined effects of thyristor control phase shifters (TCPS) and SMES in different power system models. The investigations demonstrate that by installing a TCPS in conjunction with SMES units in each area, the dynamic response of the system is significantly improved. However, the investigations were limited to deregulated power systems and were limited to interconnected power systems having identical reheat or non-reheat turbines, and little focus is given to interconnected power systems with different generating turbines that have vastly different characteristics, therefore, there is a need for further research in this area.

Given the above discussion, this article subsequently presents the design of an optimal controller for frequency and tie-line power stability, based on formulating an error value and finding the feedback gains corresponding to each state of the system. It is based on error minimization for interconnected power systems. The impact of DFIG (with and without TCPS-SMES) in restoring optimum system frequency, for sudden load fluctuations in an interconnected system, is analyzed. The investigations are verified by calculating the performance index value, the closed ring real and imaginary values, finding the feedback gains, and through graphical simulations of the three system models under investigation.

2. MODEL UNDER STUDY

The following power system models are analyzed: i) Framework model-1: a two-area interconnected power system with hydro generation in area 1 and tandem compound non-reheat turbines in area two. The two areas are interconnected through an AC tie-line, ii) Framework model-2: is a replica of model one but the two areas interconnected by the AC tie-line are supported by DFIG-based wind turbines in each area. iii) Framework model-3: is a replica of model 2 but the interconnected system employs TCPS in series with the AC tie-line with a SMES unit located in area two of the system. The data for the non-reheat turbines and the DFIG-based wind turbines are provided in the Appendix. The model is shown in Figure 1.
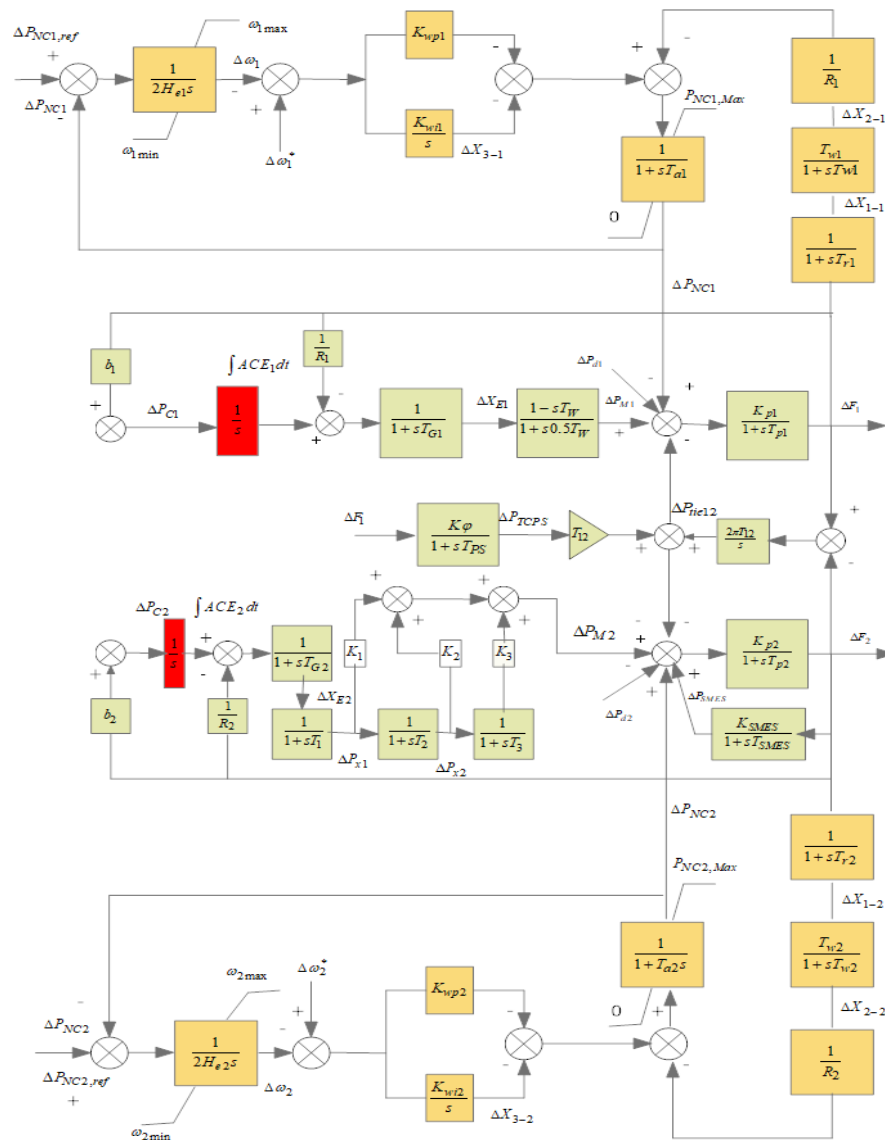

Figure 1. Interlinked model of a hydro plant and a thermal plant having tandem compound non-reheat turbines with DFIG and TCPS-SMES

3.   MODELLING OF WIND SYSTEM INCORPORATING DFIG

When wind generators are employed in frequency control, the wind turbines do not supply their accessible power directly into the system, thereby maintaining a reserve for frequency control. Variable speed generators coupled to the wind turbines are used to extract the kinetic energy stored in the mechanical system. To achieve frequency control, DFIG-based wind turbines can deliver power with variable mechanical speeds allowing for the kinetic energy to be extracted [18]. The transfer function model, shown in Figure 2, employs DFIG-based wind generators in each area for active power control [19]. The model has the essence of emulation inertial control (EIC). In the EIC of a DFIG, a second control loop is utilized to adjust the control reference points as a function of frequency change and rate of frequency change. To produce maximum power, the controllers try to maintain optimal turbine speed. The controller provides a power reference point based on measured speed and measured electrical power. The second loop is activated when the grid frequency exceeds predetermined limits. When the system frequency decreases, the reference torque is increased, allowing for the rotor to decrease speed and distribute the kinetic energy. DFIGs utilize their' kinetic energy in response to frequency variations during load fluctuations. The active power supplied by the wind turbine amid any load fluctuations is ΔP_{NC}. The power supplied is compared with ΔP_{NCref} for maximum output power. This is achieved by keeping rotor reference speed where maximum power is attained. The mechanical power captured by the wind turbine is given by (1). The development of the transfer function model of a DFIG-based wind turbine participating in frequency stability during load fluctuations is well covered in [18]. Mathematical modeling of TCPS-SMES is available in [34]. However, the dynamics of TCPS-SMES are not covered at appropriate place intervals in the form of gain and time constants to evaluate their impact in reaching the original frequency of the system.

$$P_{mech} = (\frac{\frac{1}{2}(\rho Ar)}{S_n} C_{p.opt})\omega_s^3 \qquad (1)$$
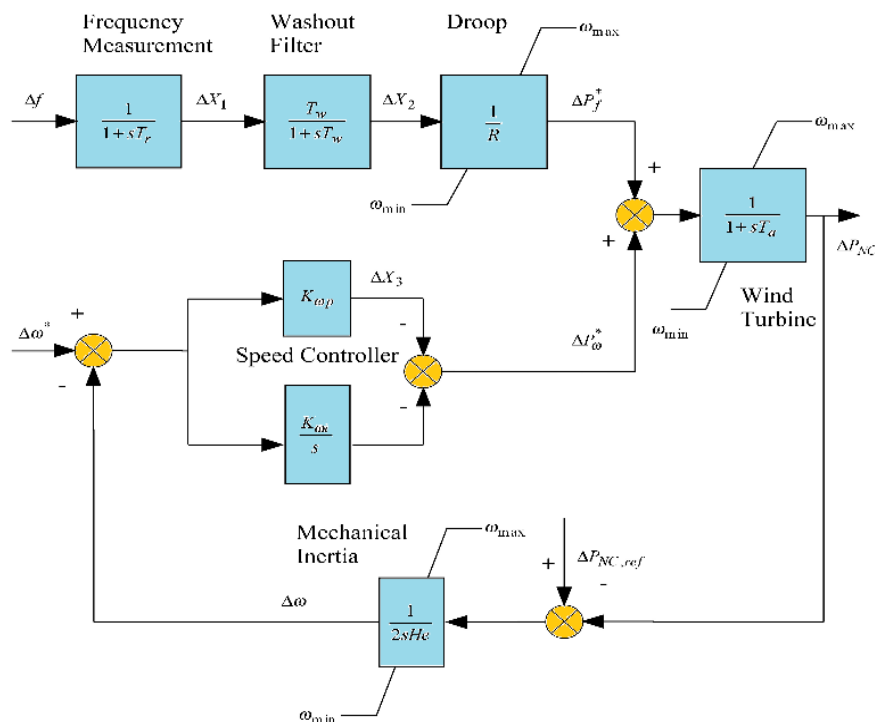

Figure 2. Schematic of the DFIG

4.   DETAILED MODELLING OF OPTIMAL CONTROL

An s-area interconnected power system is represented by a direct time-invariant system within the state variable form:

$$\frac{d}{dt}(X) = AX + BU + \Gamma P_d , \qquad (2)$$

$$Y = CX \tag{3}$$

the control flag U is such that it minimizes the execution file (J) given by:

$$j = \int_0^\infty \frac{1}{2}[\,X^T Q X + \, U^T R U]dt \tag{4}$$

within the application of an ideal control hypothesis, the term ΓPd in (2) can be eliminated by reclassifying the states and controls in terms of their steady-state values occurring after the fluctuation. (2) can be modified as:

$$\frac{d}{dt}(X) = AX + BU + \Gamma P_d \,, X(0) = X_0 \tag{5}$$

and (3) will remain the same. With a full state vector, a control law is expressed within the frame:

$$U^* = -[\Psi^*]X \tag{6}$$

this minimizes the execution given by (4). For the continuous time issue, the application of pontryagin's minimum principle is applied to reduce the network to its riccati condition:

$$PA + A^T P - PBR^{-1}B^T P + Q = 0 \tag{7}$$

the arrangement of (7) yields a positive clear symmetric matrix, P, and the ideal control law is given:

$$U^* = -R^{-1}B^T PX \tag{8}$$

the optimal system matrix with complete feedback gain is (9).

$$[\psi^*] = R^{-1}B^T P \tag{9}$$

5. RESULTS AND DISCUSSION

The optimal controller is designed for the system as illustrated in Figure 1 for a two-area interconnected power system with active support from DFIG-based wind turbines in each area. In area one, the power is generated by hydropower. In area two the power is generated through tandem compound non-reheat turbines. The two areas are linked via an AC tie-line. In addition to this, the effect of TCPS in series on the AC tie-line and SMES unit installed in area two is investigated, to determine its impact in restoring the optimum system frequency after sudden load fluctuations. The optimal control strategy is developed by considering each state of the power system models. To implement the optimal control action for the three power system models, the output of the controller is verified based on performance index minimization, closed ring eigenvalues, and computed feedback gains. The system frequency analysis is done based on a 1% load fluctuation in the hydropower plant. The analysis is done through results obtained in Tables 1-3.

The data in Table 1 shows the performance index (PI) values for the three power system models. For optimal FC the PI value is 13.1619. The PI value for optimal FC is reduced from 13.1619 to 1.1668 with wind power integration utilizing DFIG in each area of the interconnected system. This demonstrates the positive impact of DFIG-based wind power integration in each area. However, the PI value is further reduced from 1.1668 to 1.0203 when TCPS is linked in series to the AC tie-line with a SMES unit installed in area two of the interconnected system. The feedback gains for each state for the three power system models are shown in Table 2. It is noted that feedback gains increase with each subsequent model; from optimal FC to optimal FC with DFIG and further to optimal FC with DFIG and TCPS-SMES. The closed-loop eigenvalues of the three power system models are shown in Table 3. The review of the closed-loop eigenvalues demonstrates that closed-loop system stability is guaranteed for all system state scenarios. The eigenvalues indicate that the real and imaginary components of the system increase progressively when DFIG is installed in each area of the interconnected power system. Further progression is achieved in the real and imaginary components of eigenvalues when the dynamics of TCPS and SMES are considered in conjunction with DFIG in the interconnected hydro-thermal power system. This guarantees the steady state and dynamic output for optimal FC for the interconnected power system in restoring the optimum frequency of the system after sudden load fluctuations.

Table 1. Optimum PI values

| Optimal FC	Optimal FC+DFIG	Optimal FC+DFIG+TCPS-SMES
13.1619	1.1668	1.0203

Table 2. Feedback gains from various developed systems

Optimal FC	Optimal FC+DFIG	Optimal FC+DFIG+TCPS-SMES
[0.9889 2.0820 0.2825 1.2375 -0.0644 0.1483 0.0375 -0.0788 0.4989 0.3715 -0.0300; -0.1483 0.1046 0.0448 0.1794 1.4592 0.9889 0.7327 0.0267 2.1291 1.5838 0.5870]	[0.9963 2.2476 0.3360 1.3053 -0.8969 0.4171 -0.6392 - 1.7431 1.3925 -2.9097 0.0863 -0.0034 -0.0281 0.2336 0.0484 - 0.0915 0.1691 -0.1648 - 0.5303 -0.0703 -0.8312; -0.0863 0.0684 0.0312 0.1315 1.3494 0.0041 - 0.0112 -0.1275 0.0649 - 0.1863 0.9963 0.6901 0.0014 1.6826 1.6579 0.5722 0.9308 -1.0779 - 2.8589 0.8328 -5.0095]	[0.9919 2.4661 0.4109 1.4889 -1.2684 0.4321 -0.6824 -1.8396 1.5936 -3.0604 0.1270 0.0194 0.0388 0.1534 0.2225 0.0464 0.0940 -0.1181 -0.4178 0.0853 -0.6638 0.0349 -0.0070; -0.1270 0.0879 0.0374 0.1445 0.6438 0.0142 -0.0253 -0.1445 0.0865 -0.2078 0.9919 0.6562 0.0393 1.5926 1.3274 0.4150 0.8594 -0.9660 -2.5817 0.6251 -4.5781 -0.0402 -0.0875]

Table 3. Eigenvalues analysis

Optimal FC	Optimal FC+DFIG	Optimal FC+DFIG+TCPS-SMES
-35.4798+0.0000i	-35.5300+0.0000i	-35.5709+0.0000i
-11.1466+0.0000i	-11.1796+1.7455i	-32.5896+0.0000i
-6.1515+0.9164i	-11.1796-1.7455i	-11.7485+0.0000i
-6.1515-0.9164i	-11.6357+0.0000i	-10.1995+1.8141i
-3.3127+0.0000i	-6.4103+1.4819i	-10.1995-1.8141i
-1.0758+2.3560i	-6.4103-1.4819i	-5.6829+4.0859i
-1.0758-2.3560i	-4.2347+3.7554i	-5.6829-4.0859i
-2.4821+0.0000i	-4.2347-3.7554i	-6.4152+1.4772i
-0.4061+0.0000i	-1.6916+3.8277i	-6.4152-1.4772i
-0.3059+0.1820i	-1.6916-3.8277i	-10.0000+0.0000i
-0.3059-0.1820i	-2.4382+0.0000i	-1.9851+4.0339i
	-1.0812+0.0000i	-1.9851-4.0339i
	-0.4888+0.3019i	-2.4499+0.0000i
	-0.4888-0.3019i	-0.7673+0.0000i
	-0.4137+0.0000i	-0.4969+0.3241i
	-0.2287+0.0000i	-0.4969-0.3241i
	-0.1862+0.0281i	-0.4397+0.0000i
	-0.1862-0.0281i	-0.2093+0.0000i
	-0.1667+0.0000i	-0.1776+0.0341i
	-0.1000+0.0000i	-0.1776-0.0341i
	-0.1000+0.0000i	-0.1668+0.0000i
		-0.1000+0.0000i
		-0.1000+0.0000i

The restoration curves for the optimal FC are shown in Figures 3 and 4, for various outputs of the model, and a comparative analysis of the framework models is shown. Figures 3(a)-3(b) show the frequency variations in areas one and two, respectively. It was observed that the frequency variations in both areas were comparatively large with only the optimal control action. With the active contribution of the DFIG-based wind turbines and the support of the TCPS-SMES, the frequency variations progressively reduced in area one but in area two there was a quick and drastic reduction. Figures 3(c)-3(d) show the tie-line power variations and the area control error respectively. It is observed that, with the active participation of the DFIG-based wind turbines and the TCPS-SMES, the tie-line power deviation is reduced, with a smoother restoration curve and faster settling times, and the ACE error is also reduced. Figures 4(a)-4(b) show the frequency variations in areas one and two respectively, with a 1% load alteration in the hydro power plant and a 2% load change in the thermal power plant. Figures 4(c)-4(d) show the tie-line power variations and the control error in area one respectively. From Figures 4(a)-4(d) it is observed that the area frequencies and tie-line power variations are greater compared to those observed in Figures 3(a)-3(d), which is expected due to the additional load increase in area two.
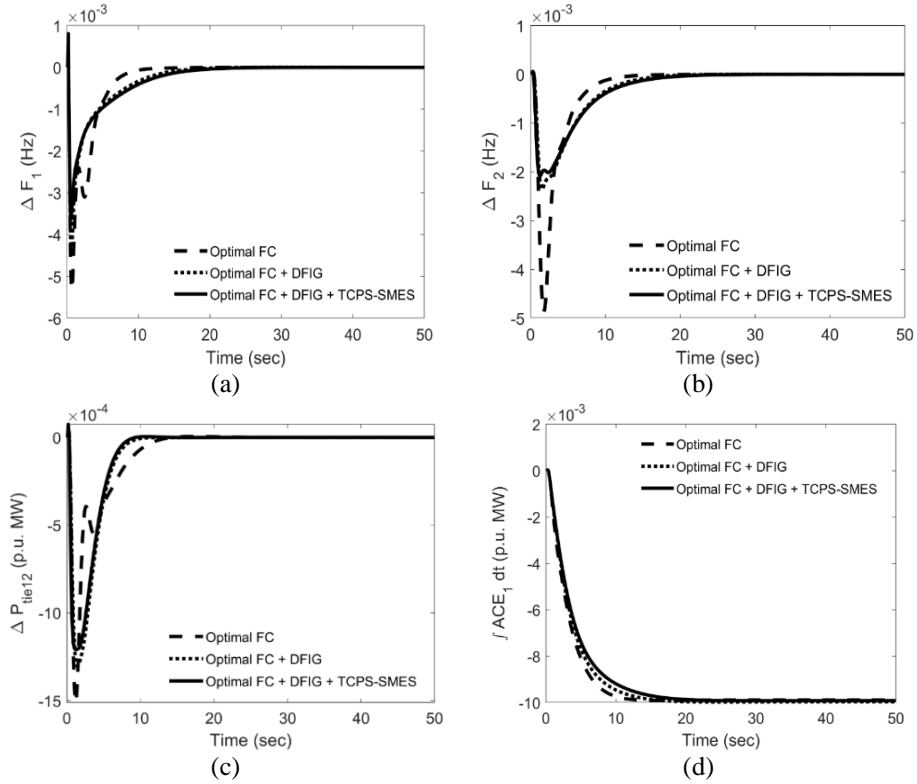
Figures 3. Results for a 1% load alteration in the hydro power plant; (a) area 1 frequency restoration, (b) area 2 frequency restoration, (c) tie line power restoration, and (d) ACE
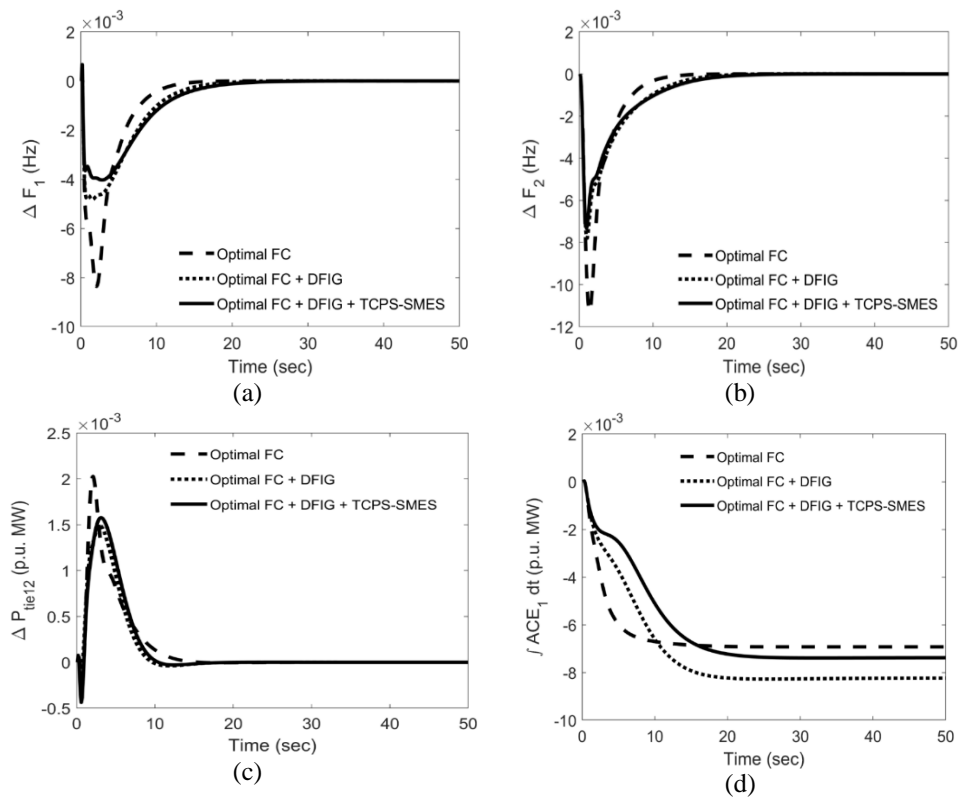
Figures 4. Results for 1% load alteration in the hydro plant and 2% load change in the thermal power plant; (a) area 1 frequency restoration, (b) area 2 frequency restoration, (c) tie line power restoration, and (d) ACE

The results demonstrate that wind power integration with DFIG-based wind turbines can store excessive generated power from the rotor of the generators when there is excessive power available in the system. This excessive power can immediately contribute to the interconnected power system when the load demand exceeds the generation capacity. This allows for the system to reach optimum system frequency with reduced overshoot and faster response times. Further, it is also observed that the DFIG in conjunction with the pair of TCPS-SMES improves the capability of the controller to restore the optimal frequency of the system with a lower first peak, oscillation-free system results, and faster steady state performance of the interconnect power system.

6. CONCLUSION

This paper showed an initial attempt to link the DFIG-based wind turbines in an interconnected hydro-thermal power system with hydro turbines in zone one and tandem compound-built non-reheat turbine base thermal generation in zone two. The two zones are linked via an AC tie-line. The different framework models were developed in this study to investigate the impact of DFIG in interconnected hydro-thermal systems. In addition to the installation of DFIG in each zone, the TCPS connected in series to the AC tie-line and SMES linked in zone two of the power was also investigated. The optimal frequency controller was designed and simulated to achieve optimal frequency and tie-line power stability for load fluctuations in an interconnected system. The outputs of framework models were evaluated based on error value, feedback gains, and eigenvalues and via graphical results. The outputs demonstrated that DFIG linked in each zone of the hydro-thermal system reduced the error value appreciably. It was also observed that the real and imaginary values of the closed ring increased numerically and hence it improved the steady state and dynamic output of the system. Further, when TCPS-SMES dynamics were included in the framework model with DFIG, the error was reduced further and the eigenvalues improved significantly, hence enhancing the stability of the interconnected system. From graphical results, it was seen that the optimal frequency controller has a lower overshoot and faster settling times to the original values of all system states, after sudden load fluctuations when DFIG with TCPS-SMES is installed in the interconnected hydro-thermal system.

APPENDIX
Numerical date;
$P_{r1} = P_{r2} = 2000\ MW, T_{G1} = 0.08\ s, T_{G2} = 0.2\ s, R_1 = R_2 = 2.5\ Hz/p.uMW, T_w = 0.1s, T_1 = 0.2s,$
$T_2 = 6\ s, T_3 = 0.4\ s, K_1 = 0.3, K_2 = 0.4, K_3 = 0.3, b_1 = b_2 = 0.425\ p.u.MW/Hz,$
$\Delta P_{d1} = \Delta P_{d2} = 0.01\ p.u.MW, K_{p1} = K_{p2} = 120\ Hz(p.u.MW), T_{p1} = T_{p2} = 20s$

Data for DFIG-based wind turbines;
$H_{e1} = H_{e2} = 3.5\ p.u.MW.s, K_{\omega p1} = K_{\omega p2} = 1, K_{\omega i1} = K_{\omega i2} = 0.5, T_{a1} = T_{a2} = 0.2s, T_{r1} = T_{r2} = 15s,$
$T_{w1} = T_{w2} = 6s$

REFERENCES
[1] O. I. Elgerd and C. E. Fosha, "Optimum megawatt-frequency control of multiarea electric energy systems," *IEEE Transactions on Power Apparatus and Systems*, vol. PAS-89, no. 4, pp. 556–563, Apr. 1970, doi: 10.1109/TPAS.1970.292602.
[2] J. L. Willems, "Sensitivity analysis of the optimum performance of conventional load-frequency control," *IEEE Transactions on Power Apparatus and Systems*, vol. PAS-93, no. 5, pp. 1287–1291, Sep. 1974, doi: 10.1109/TPAS.1974.293852.
[3] A. Panwar, G. Sharma, S. K. Sahoo, and R. C. Bansal, "Active power regulation of hydro dominating energy system using IDD optimized FPA," *Energy Procedia*, vol. 158, pp. 6328–6333, Feb. 2019, doi: 10.1016/j.egypro.2019.01.356.
[4] S. K. Sahoo, G. Sharma, A. Panwar, and R. C. Bansal, "Frequency regulation of wind integrated power system using dual mode fuzzy," *Energy Procedia*, vol. 158, pp. 6321–6327, Feb. 2019, doi: 10.1016/j.egypro.2019.01.381.
[5] Ibraheem and P. Kumar, "Current status of the Indian power system and dynamic performance enhancement of hydro power systems with asynchronous tie lines," *Electric Power Components and Systems*, vol. 31, no. 7, pp. 605–626, Jul. 2003, doi: 10.1080/15325000390203638.
[6] T. H. Mohamed, H. Bevrani, A. A. Hassan, and T. Hiyama, "Decentralized model predictive based load frequency control in an interconnected power system," *Energy Conversion and Management*, vol. 52, no. 2, pp. 1208–1214, Feb. 2011, doi: 10.1016/j.enconman.2010.09.016.
[7] V. Chandrakala, B. Sukumar, and K. Sankaranarayanan, "Load frequency control of multi-source multi-area hydro thermal system using flexible alternating current transmission system devices," *Electric Power Components and Systems*, vol. 42, no. 9, pp. 927–934, Jul. 2014, doi: 10.1080/15325008.2014.903540.
[8] Tarkeshwar and V. Mukherjee, "A novel quasi-oppositional harmony search algorithm and fuzzy logic controller for frequency stabilization of an isolated hybrid power system," *International Journal of Electrical Power and Energy Systems*, vol. 66, pp. 247–261, Mar. 2015, doi: 10.1016/j.ijepes.2014.10.050.
[9] P. Bhatt, R. Roy, and S. P. Ghoshal, "Dynamic participation of doubly fed induction generator in automatic generation control," *Renewable Energy*, vol. 36, no. 4, pp. 1203–1213, Apr. 2011, doi: 10.1016/j.renene.2010.08.017.

[10] G. Sharma, "Optimal AGC design for diverse sources of power generations in each area using output vector feedback control technique," *International Journal of Engineering Research in Africa*, vol. 45, pp. 99–114, Nov. 2019, doi: 10.4028/www.scientific.net/JERA.45.99.

[11] Ibraheem, K. R. Niazi, and G. Sharma, "Study on dynamic participation of wind turbines in automatic generation control of power systems," *Electric Power Components and Systems*, vol. 43, no. 1, pp. 44–55, Jan. 2015, doi: 10.1080/15325008.2014.963266.

[12] K. P. S. Parmar, S. Majhi, and D. P. Kothari, "LFC of an interconnected power system with multi-source power generation in deregulated power environment," *International Journal of Electrical Power and Energy Systems*, vol. 57, pp. 277–286, May 2014, doi: 10.1016/j.ijepes.2013.11.058.

[13] Y. Arya and N. Kumar, "AGC of a multi-area multi-source hydrothermal power system interconnected via AC/DC parallel links under deregulated environment," *International Journal of Electrical Power & Energy Systems*, vol. 75, pp. 127–138, Feb. 2016, doi: 10.1016/j.ijepes.2015.08.015.

[14] Y. Arya, N. Kumar, and Ibraheem, "AGC of a two-area multi-source power system interconnected via AC/DC parallel links under restructured power environment," *Optimal Control Applications and Methods*, vol. 37, no. 4, pp. 590–607, Jul. 2016, doi: 10.1002/oca.2181.

[15] P. K. Keung, P. Li, H. Banakar, and B. T. Ooi, "Kinetic energy of wind-turbine generators for system frequency support," *IEEE Transactions on Power Systems*, vol. 24, no. 1, pp. 279–287, Feb. 2009, doi: 10.1109/TPWRS.2008.2004827.

[16] X. Yingcheng and T. Nengling, "Review of contribution to frequency control through variable speed wind turbine," *Renewable Energy*, vol. 36, no. 6, pp. 1671–1677, Jun. 2011, doi: 10.1016/j.renene.2010.11.009.

[17] J. Ekanayake and N. Jenkins, "Comparison of the response of doubly fed and fixed-speed induction generator wind turbines to changes in network frequency," *IEEE Transactions on Energy Conversion*, vol. 19, no. 4, pp. 800–802, Dec. 2004, doi: 10.1109/TEC.2004.827712.

[18] R. G. Almeida and J. A. P. Lopes, "Participation of doubly fed induction wind generators in system frequency regulation," *IEEE Transactions on Power Systems*, vol. 22, no. 3, pp. 944–950, Aug. 2007, doi: 10.1109/TPWRS.2007.901096.

[19] M. Jalali, "DFIG based wind turbine contribution to system frequency control," Electronics and Computer Engineering, University of Waterloo, 2011.

[20] W. Qiao and R. G. Harley, "Effect of grid-connected DFIG wind turbines on power system transient stability," in *IEEE Power and Energy Society 2008 General Meeting: Conversion and Delivery of Electrical Energy in the 21st Century, PES*, Jul. 2008, pp. 1–7, doi: 10.1109/PES.2008.4596912.

[21] A. Petersson, "Analysis, modeling and control of doubly-fed induction generators for wind turbines," Chalmers University of Technology, 2005.

[22] J. C. Muñoz and C. A. Cañizares, "Comparative stability analysis of DFIG-based wind farms and conventional synchronous generators," in *2011 IEEE/PES Power Systems Conference and Exposition, PSCE 2011*, Mar. 2011, pp. 1–7, doi: 10.1109/PSCE.2011.5772545.

[23] M. Kayikçi and J. V. Milanović, "Dynamic contribution of DFIG-based wind plants to system frequency disturbances," *IEEE Transactions on Power Systems*, vol. 24, no. 2, pp. 859–867, May 2009, doi: 10.1109/TPWRS.2009.2016062.

[24] J. M. Mauricio, A. Marano, A. Gómez-Expósito, and J. L. M. Ramos, "Frequency regulation contribution through variable-speed wind energy conversion systems," *IEEE Transactions on Power Systems*, vol. 24, no. 1, pp. 173–180, Feb. 2009, doi: 10.1109/TPWRS.2008.2009398.

[25] J. J. Shea, "Understanding FACTS-concepts and technology of flexible AC transmission systems [Book Review]," *IEEE Electrical Insulation Magazine*, vol. 18, no. 1, pp. 46–46, Jan. 2005, doi: 10.1109/mei.2002.981326.

[26] T. M. L. Assis, E. H. Watanabe, L. A. S. Pilotto, and R. B. Sollero, "A new technique to control reactive power oscillations using STATCOM," in *10th International Conference on Harmonics and Quality of Power. Proceedings (Cat. No.02EX630)*, 2004, vol. 2, pp. 607–613, doi: 10.1109/ichqp.2002.1221505.

[27] F. H. Gandoman *et al.*, "Review of FACTS technologies and applications for power quality in smart grids with renewable energy systems," *Renewable and Sustainable Energy Reviews*, vol. 82, pp. 502–514, Feb. 2018, doi: 10.1016/j.rser.2017.09.062.

[28] I. A. Chidambaram and B. Paramasivam, "Optimized load-frequency simulation in restructured power system with redox flow batteries and interline power flow controller," *International Journal of Electrical Power and Energy Systems*, vol. 50, no. 1, pp. 9–24, Sep. 2013, doi: 10.1016/j.ijepes.2013.02.004.

[29] H. J. Kunisch, K. G. Kramer, and H. Dominik, "Battery energy storage another option for load-frequency-control and instantaneous reserve," *IEEE Transactions on Energy Conversion*, vol. EC-1, no. 3, pp. 41–46, Sep. 1986, doi: 10.1109/TEC.1986.4765732.

[30] S. Kalyani, S. Nagalakshmi, and R. Marisha., "Load frequency control using battery energy storage system in interconnected power system," in *2012 3rd International Conference on Computing, Communication and Networking Technologies, ICCCNT 2012*, Jul. 2012, pp. 1–6, doi: 10.1109/ICCCNT.2012.6396052.

[31] S. C. Tripathy, R. Balasubramanian, and P. S. C. Nair, "Adaptive automatic generation control with superconducting magnetic energy storage in power systems," *IEEE Transactions on Energy Conversion*, vol. 7, no. 3, pp. 434–441, 1992, doi: 10.1109/60.148563.

[32] S. C. Tripathy, R. Balasubramanian, and P. S. C. Nair, "Effect of superconducting magnetic energy storage on automatic generation control considering governor deadband and boiler dynamics," *IEEE Transactions on Power Systems*, vol. 7, no. 3, pp. 1266–1273, 1992, doi: 10.1109/59.207343.

[33] S. C. Tripathy and K. P. Juengst, "Sampled data automatic generation control with superconducting magnetic energy storage in power systems," *IEEE Transactions on Energy Conversion*, vol. 12, no. 2, pp. 187–192, Jun. 1997, doi: 10.1109/60.629702.

[34] P. Bhatt, S. P. Ghoshal, and R. Roy, "Coordinated control of TCPS and SMES for frequency regulation of interconnected restructured power systems with dynamic participation from DFIG based wind farm," *Renewable Energy*, vol. 40, no. 1, pp. 40–50, Apr. 2012, doi: 10.1016/j.renene.2011.08.035.

[35] P. Bhatt, R. Roy, and S. P. Ghoshal, "Comparative performance evaluation of SMES-SMES, TCPS-SMES and SSSC-SMES controllers in automatic generation control for a two-area hydro-hydro system," *International Journal of Electrical Power and Energy Systems*, vol. 33, no. 10, pp. 1585–1597, Dec. 2011, doi: 10.1016/j.ijepes.2010.12.015.

[36] P. Bhatt, S. P. Ghoshal, and R. Roy, "Load frequency stabilization by coordinated control of thyristor controlled phase shifters and superconducting magnetic energy storage for three types of interconnected two-area power systems," *International Journal of Electrical Power and Energy Systems*, vol. 32, no. 10, pp. 1111–1124, Dec. 2010, doi: 10.1016/j.ijepes.2010.06.009.

[37] P. Bhatt, S. P. Ghoshal, R. Roy, and S. Ghosal, "Load frequency control of interconnected restructured power system along with DFIG and coordinated operation of TCPS-SMES," in *2010 Joint International Conference on Power Electronics, Drives and Energy Systems, PEDES 2010 and 2010 Power India*, Dec. 2010, pp. 1–6, doi: 10.1109/PEDES.2010.5712524.

BIOGRAPHIES OF AUTHORS

Nelson Dhanpal Chetty is a Lecturer in the Department of Electrical Power Engineering, Durban University of Technology, South Africa, and is presently working towards his Ph.D. at the Department of Electrical and Electronics Engineering, University of Johannesburg, South Africa. He has a B. Tech and M.Eng. qualifications from the Department of Electrical Power Engineering, Durban University of Technology. His area of interest includes power system operation and control, renewable energy technology, and optimization techniques. He can be contacted at email: nelsonc@dut.ac.za.

Gulshan Sharma is a Senior Lecturer in the Department of Electrical Engineering Technology at the University of Johannesburg. He has a B. Tech, M. Tech, and Ph.D. qualifications. He is an Academic Editor of the International Transactions on Electrical Energy System Journal, Wiley. He is a Y-rated researcher from NRF South Africa. His area of interest includes power system operation and control and the application of AI techniques to power systems. He can be contacted at email: gulshans@uj.ac.za.

Pitshou N. Bokoro is a member of IEEE. He received a BTech (Electrical) degree and a M.Phil. in electrical engineering from the University of Johannesburg, in 2011, and a Ph.D. degree in electrical engineering from the University of the Witwatersrand, in 2016. He is currently an Associate Professor in the Faculty of Engineering and the Built Environment (FEBE) of the University of Johannesburg. His research interests include power quality, power systems optimization, condition monitoring (diagnosis and prognosis) reliability prediction of insulating materials and dielectrics, surge protection, and renewable energies. He is a senior member of the South African Institute of Electrical Engineers and a member of the Institute of Electrical and Electronic Engineers (IEEE). He can be contacted at email: pitshoub@uj.ac.za.

Manoj Kumawat is an Assistant Professor in the Department of Electrical Engineering at, the National Institute of Technology, Delhi, India. He has the qualifications of B. Tech, M. Tech, and Ph.D. from institutes of national prominence in India. His research area includes power system operation and control, optimization techniques, renewable energy technologies, and the application of AI techniques to power systems. He can be contacted at email: manoj@nitdelhi.ac.in.